Target Penetration of Laser-Based 3D Imaging Systems

Geraldine S. Cheok*[a], Kamel S. Saidi[a], Marek Franaszek[a]

[a]National Institute of Standards and Technology, 100 Bureau Dr, Gaithersburg, MD, USA 20899

ABSTRACT

The ASTM E57.02 Test Methods Subcommittee is developing a test method to evaluate the ranging performance of a 3D imaging system. The test method will involve either measuring the distance between two targets or between an instrument and a target. The first option is necessary because some instruments cannot be centered over a point and will require registration of the instrument coordinate frame into the target coordinate frame. The disadvantage of this option is that registration will introduce an additional error into the measurements. The advantage of this option is that this type of measurement, relative measurement, is what is typically used in field applications. A potential target geometry suggested for the test method is a planar target. The ideal target material would be diffuse, have uniform reflectivity for wavelengths between 500 nm to 1600 nm (wavelengths of most commercially-available 3D imaging systems), and have minimal or no penetration of the laser into the material. A possible candidate material for the target is Spectralon[1]. However, several users have found that there is some penetration into the Spectralon by a laser and this is confirmed by the material manufacturer. The effect of this penetration on the range measurement is unknown. This paper will present an attempt to quantify the laser penetration depth into the Spectralon material for four 3D imaging systems.

Keywords: 3D imaging systems, diffuse, laser, material penetration, retroreflectance.

1. INTRODUCTION

ASTM E57 committee was established in 2006 and is charged with developing standards for 3D imaging systems [1, 2]. The ASTM E57.02 Test Methods Subcommittee is developing a test method to evaluate the ranging performance of a 3D imaging system [such as laser scanners, LADAR (laser detection and ranging)] [3]. As there are currently no standards for 3D imaging systems, this standard test method will provide a means to objectively evaluate the range performance of these systems. The basic idea of the protocol is the comparison of distances as measured by the 3D imaging system to "truth". The test method will involve measuring the distance between two targets or between an instrument and a target. The former is necessary because some instruments cannot be centered over a point and will require registration of the instrument coordinate frame into the target coordinate frame. The disadvantage of this option is that registration will introduce an additional error into the measurements. The advantage of this type of measurement, relative distance, is that it is what is typically used in field applications.

As with any standard method, repeatability of the method is essential. Therefore, if the method specifies the use of a target, then the target should be standard, i.e., the properties of the target should be the same for all instruments or that the target should be characterized for the instrument being evaluated. The preference is the former option as it will not involve additional steps and the results will be directly comparable. A potential target suggested for the test method is a planar target. The ideal target would:

- be diffuse - that is, reflectivity does not change with angle of incidence of the laser beam;

- have uniform reflectivity for wavelengths between 500 nm to 1600 nm (wavelengths of most commercially-available 3D imaging systems) - that is, the reflectivity of the material should not be 80 % for $\lambda = 600$ nm and 95 % for $\lambda = 1500$ nm; and

- have no penetration of the laser into the material.

---

[1] Certain trade names and company products are mentioned in the text or identified in an illustration in order to adequately specify the experimental procedure and equipment used. In no case does such an identification imply recommendation or endorsement by the National Institute of Standards and Technology, nor does it imply that the products are necessarily the best available for the purpose.

A possible candidate material for the target is Spectralon which exhibits two of these properties. Spectralon is a thermoplastic resin and is a Lambertian surface. However, several users have found that there is some penetration into the Spectralon by a laser. The manufacturer of Spectralon confirmed that Spectralon does have a 99 % penetration depth of about 3 mm - that is, 99 % of the light does not travel more than 3 mm into the surface before it is returned to the surface to be re-emitted. The effect of this penetration on the range measurement is unknown. This paper presents an attempt to quantify the effect of the penetration into the Spectralon material on the range measurement for four 3D imaging systems.

2. EXPERIMENT

2.1 Description of experiment

The general approach used in the experiment was to compare the measurements of a Spectralon plate made with a 3D imaging system to measurements of another material made with the same system. After some discussion within ASTM E57.02, the group decided that an aluminum plate was a possible candidate since 1) aluminum had minimal penetration, 2) the aluminum plate can be sand-blasted to make the surface diffuse, and 3) the cost was relatively inexpensive (as compared to Spectralon).

As the transmit and receive axes of the laser for most laser-based 3D imaging systems are collinear or almost collinear, the material characteristic of interest is the retroreflectance. The retroreflectance of a piece of vapor-blasted (similar to sand-blasted) aluminum was measured, and the data are shown in Figs. 1 and 2. The coefficient of retroreflected radiance for an ideal diffuser would have a value of $1/\pi$ for any angle of incidence and any observation angle. The data in Figs. 1 and 2 indicate that although the retroreflectance decreases as the angle of incidence increases, vapor-blasted aluminum is as good as most commonly used diffusers.
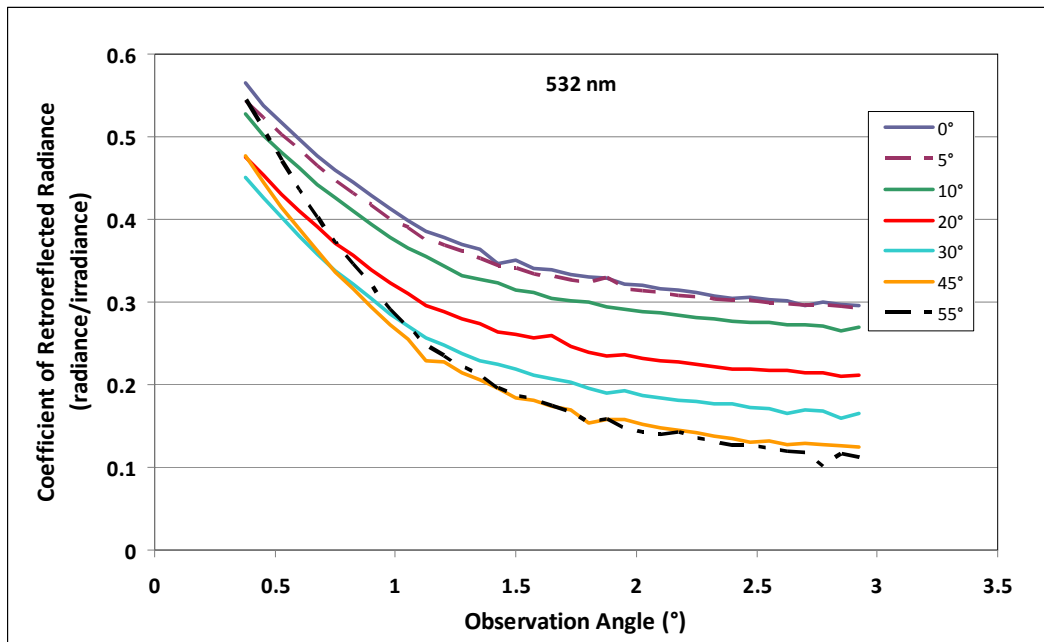

Fig. 1. Retroreflectance for a laser with $\lambda = 532$ nm for vapor-blasted aluminum. The observation angle is equal to the illuminating axis minus the observation axis. The different lines in the figure correspond to different incident angles. (Data courtesy of C. Miller, NIST)
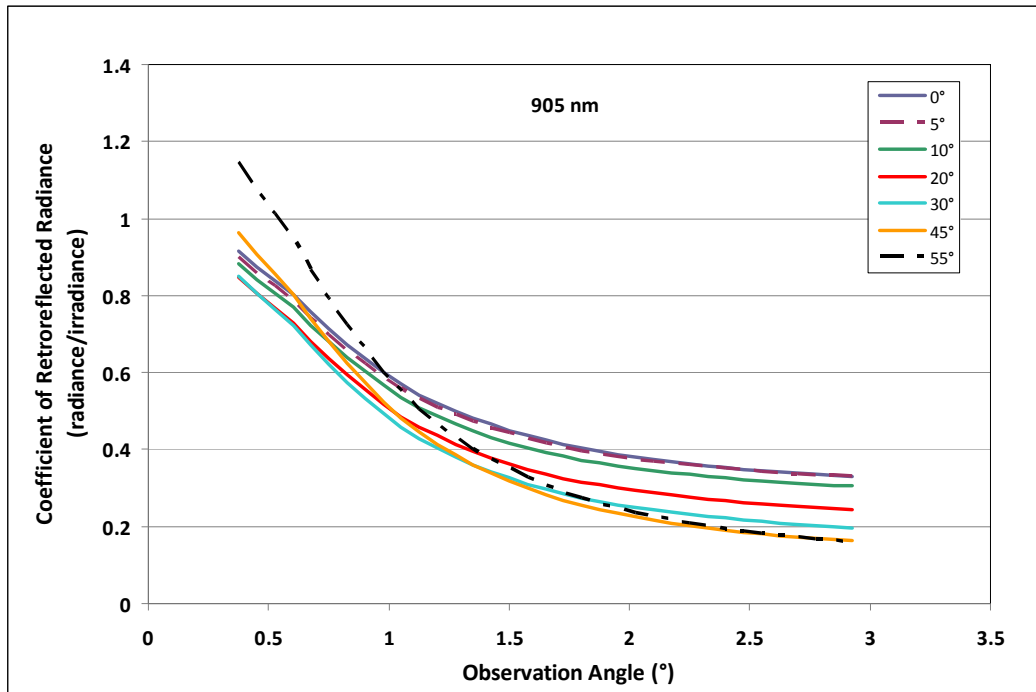
Fig. 2. Retroreflectance for a laser with λ = 905 nm for vapor-blasted aluminum. The observation angle is equal to the illuminating axis minus the observation axis. The different lines in the figure correspond to different incident angles. (Data courtesy of C. Miller, NIST)

Based on this observation, a piece of Spectralon (> 90 % reflective), 114 mm x 114 mm, was placed next to a sand blasted aluminum plate (see Fig. 3) and both plates were measured with four different 3D imaging systems - Instrument 1, Instrument 2, Instrument 3, Instrument 4. Instrument 4 is a handheld 3D imaging system and the data for Instrument 4 was obtained in October 2008 - several months after the experiments were conducted for Instruments 1, 2, and 3 and by a different operator. The major factors affecting penetration of a laser into a material are the laser's wavelength and the material's properties. In this experiment, the material properties were kept constant and the laser wavelength was varied.

The wavelengths of the lasers for the instruments were 1550 nm for Instruments 1 and 3, 532 nm for Instrument 2, and 655 nm for Instrument 4. These instruments were selected because of the different wavelengths of the lasers, different specified manufacturer accuracies, and instrument availability. Two of the instruments used a laser with the same wavelength but had different stated accuracies as it would allow a direct comparison. The manufacturer specified accuracies were: 100 μm for Instrument 1, 7 mm for Instrument 2, 10 mm for Instrument 3, and 35 μm for Instrument 4. Thus, of the four instruments, Instrument 4 is the most accurate (based on the stated accuracies).

It is generally accepted that the angle of incidence of the laser to the target affects the range measurements, and there was a concern that this effect may be amplified due to the target penetration. Therefore, the targets were scanned at five different angles of incidence (AOI): 0º, 30º, 60º, -30º, and -60º (except for Instrument 4).

Only one point spacing was used for Instrument 1 and it was set to 2 mm x 2 mm. For Instruments 2 and 3, two point densities[2] were used. For Instrument 2, the scan spacing was set to 2 mm x 2 mm at 7 m (High) and 4 mm x 4 mm at 7 m (Low). For Instrument 3, the angular increment was set to 0.004º (High) and 0.01º (Low). Only one point spacing was used for Instrument 4 and the point spacing is unknown; however, the number of points in the data sets for Instrument 4 was on the same order for Instrument 3 - high density. Point density is not expected to affect penetration into the target.

---

[2] Point spacing and point density are directly related in that as point spacing decreases, point density increases.

The distance from Instruments 1 to 3 to the plates was between 6 m to 8 m. The distance from Instrument 4 to the plates was about 0.1 m.
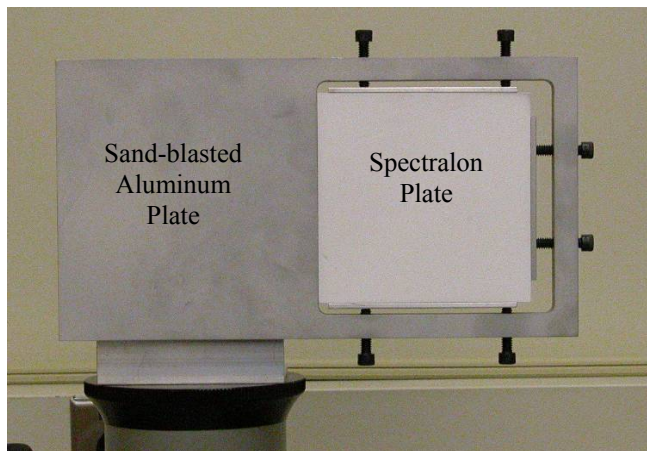

Fig. 3. Photo showing the aluminum plate and the Spectralon Plate.

2.2 Data Analysis

The data from the plate scans were manually processed so that only points in the middle of the plate were used to generate the plane representing the target. For the Instrument 3 scans, a bend in the point cloud for the aluminum points was noted when the AOI was other than 0º (see Fig. 4). Because the plate did not appear to be bent nor was the phenomenon noted in the other scans, it was concluded that the bend resulted from the instrument itself (hardware issue). A second round of segmenting the aluminum plate points was made to exclude points from the bend region. Typical point clouds for the other two instruments are shown in Figs. 5 and 6. The point clouds in Figs. 4 to 6 give a visual indication of instrument noise.
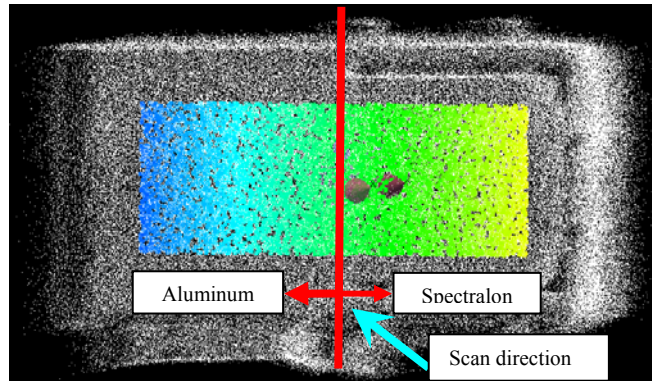
a. Front view of point cloud of aluminum-Spectralon plate. White points show the full point cloud. The colored points (point size increased for better visibility) show the points on the aluminum and Spectralon plates with the edge points removed.
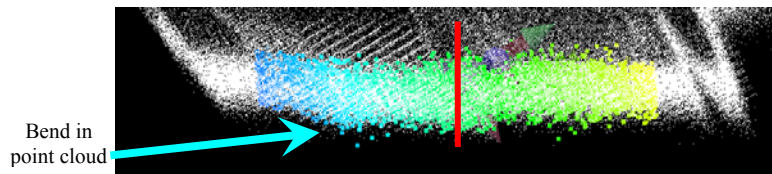
b. Top view of the point cloud of aluminum-Spectralon plate. Note bend in point cloud for the aluminum plate (left side).

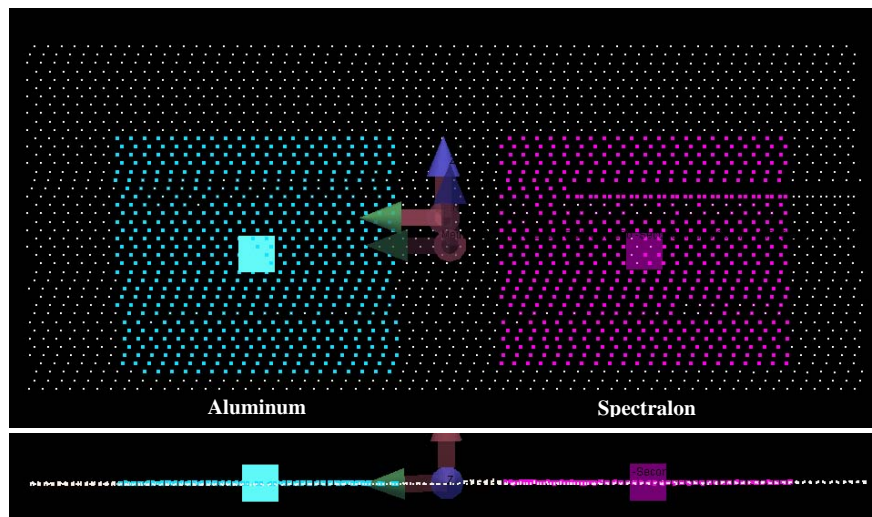Fig. 4. A point cloud for Instrument 3, AOI=30º, low density.

Fig 5. Point cloud of aluminum-Spectralon plate for a scan from Instrument 1 (scan did not extend to edges of plate). Top image shows the view from the scanner (front view) and the bottom image shows a top view of the point cloud. White points show the full point cloud. The colored points (point size increased for better visibility) show the points on the aluminum and Spectralon plates used to create the best-fit planes.
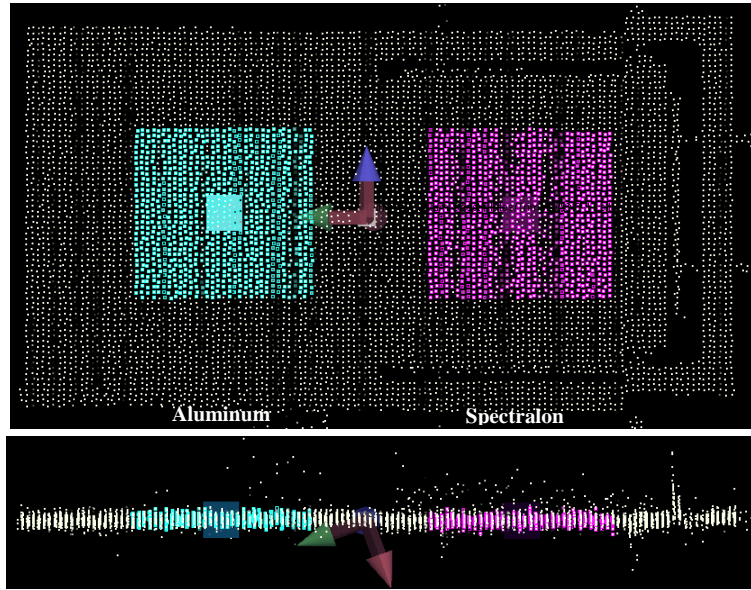
Fig 6. Point cloud of aluminum-Spectralon plate for a scan from Instrument 2. Top image shows the view from the scanner (front view) and the bottom image shows a top view of the point cloud. White points show the full point cloud. The colored points (point size increased for better visibility) show the points on the aluminum and Spectralon plates used to create the best-fit planes.

There was concern that the aluminum and Spectralon plates were not parallel. The angles between the normals of the planes for the aluminum and Spectralon plates were calculated. The average angle between the plane normals for Instrument 1 was 0.08º, for Instrument 2 was 0.37º, and for Instrument 3 was 1.74º. Since the setup of the plate was the same and the plate was not removed in between experiments, it was concluded that the increase in the angle was due to an increase in the noise of the data. Therefore, based on the data for Instrument 1[3], the plates were considered to be parallel for these experiments.

For a given instrument, AOI, and scan density, two sets of deviations were calculated. In one set, a plane was fitted through the Spectralon points, and deviations of the aluminum points to this plane were calculated (Fig. 7). In the second set, a plane was fitted through the aluminum points, and the deviations of the Spectralon points to this plane were calculated. The averages of the deviation for each of the two sets of deviations are shown in Tables 1 to 4 for Instruments 1 to 4, respectively. In the ideal case, the two values will be equal but have opposite signs. Also reported in Table 1 is the RMS of the plane fit. These values give a quantitative indication of the instrument noise.

---

[3] Instrument 4 (more accurate than Instrument 1) data was not available in time for this analysis.
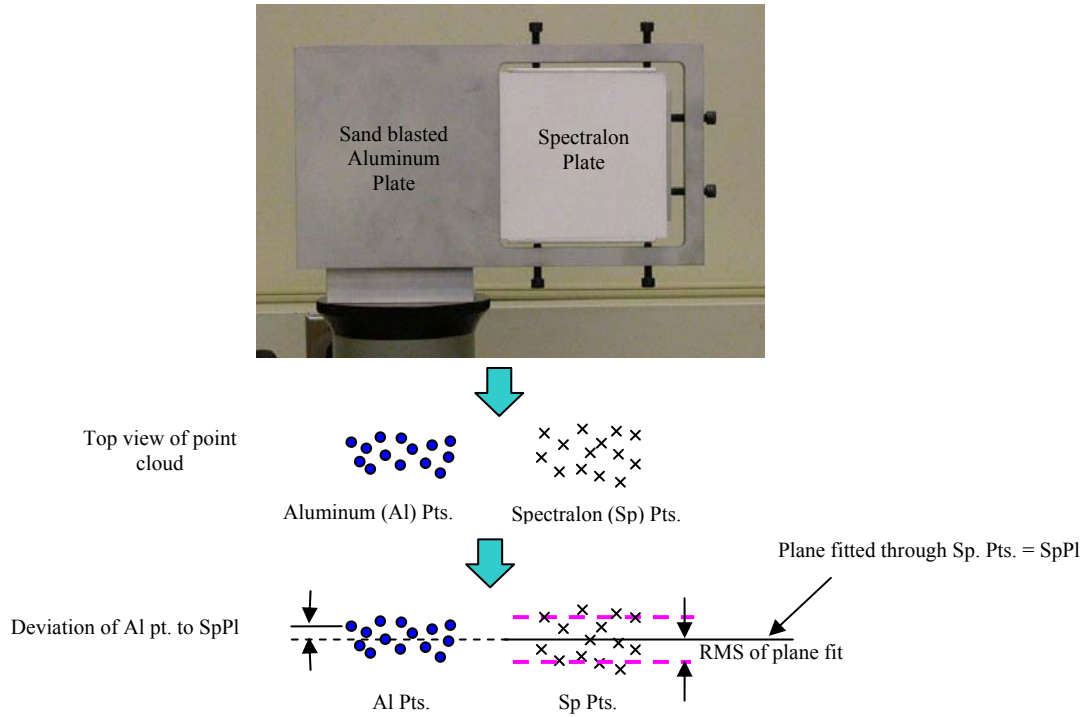
Fig. 7. Graphic showing how deviations from aluminum points to the best-fit Spectralon plane were obtained. Similarly, deviations from Spectralon points to the best-fit aluminum plane were found.

Table. 1. Instrument 1 - Deviations of points to the fitted plane. Data shown in red indicates the absolute value of the average deviation is greater than or equal to the RMS of the plane fit.

Type of Deviation	AOI (°)	Avg. Deviation (mm)	Std. Dev. Of Deviations (mm)	RMS Of Plane Fit (mm) Note: Stated instrument accuracy = 0.1 mm
Alum. pts to Sp. plane	0	0.19	0.03	0.05
Sp. pts. to alum. plane	0	-0.04	0.09	0.01
Alum. pts to Sp. plane	30	0.17	0.05	0.05
Sp. pts. to alum. plane	30	-0.02	0.09	0.03
Alum. pts to Sp. plane	60	0.14	0.08	0.05
Sp. pts. to alum. plane	60	0.03	0.12	0.05
Alum. pts to Sp. plane	-30	0.15	0.05	0.05
Sp. pts. to alum. plane	-30	-0.04	0.09	0.04
Alum. pts to Sp. plane	60	0.03	0.08	0.05
Sp. pts. to alum. plane	-60	0.03	0.11	0.05

Table. 2. Instrument 2 - Deviations of points to the fitted plane.

Type of Deviation	AOI (°)	Density	Avg. Deviation (mm)	Std. Dev. Of Deviations (mm)	RMS Of Plane Fit (mm) Note: Stated instrument accuracy = 7 mm
Alum. pts to Sp. plane	0	Low	1.3	1.5	1.4
Sp. pts. to alum. plane	0	Low	0.4	1.5	1.5
Alum. pts to Sp. plane	0	High	1.2	1.5	1.5
Sp. pts. to alum. plane	0	High	-1.1	1.5	1.5
Alum. pts to Sp. plane	30	Low	0.0	1.2	1.2
Sp. pts. to alum. plane	30	Low	0.0	1.2	1.1
Alum. pts to Sp. plane	30	High	-0.4	1.2	1.2
Sp. pts. to alum. plane	30	High	0.5	1.2	1.2
Alum. pts to Sp. plane	60	Low	-0.5	0.9	0.7
Sp. pts. to alum. plane	60	Low	0.1	0.7	0.9
Alum. pts to Sp. plane	60	High	0.6	0.9	0.7
Sp. pts. to alum. plane	60	High	-0.2	0.7	0.9
Alum. pts to Sp. plane	-30	Low	-0.7	1.2	1.2
Sp. pts. to alum. plane	-30	Low	0.0	1.2	1.2
Alum. pts to Sp. plane	-30	High	0.0	1.2	1.2
Sp. pts. to alum. plane	-30	High	-0.3	1.2	1.2
Alum. pts to Sp. plane	-60	Low	0.0	0.9	0.7
Sp. pts. to alum. plane	-60	Low	-0.7	0.7	0.9
Alum. pts to Sp. plane	-60	High	-0.2	0.7	0.9
Sp. pts. to alum. plane	-60	High	0.3	0.9	0.7

Table. 3. Instrument 3 - Deviations of points to the fitted plane. Data shown in red indicates the absolute value of the average deviation is greater than or equal to the RMS of the plane fit.

Type of deviation	AOI (°)	Density	Avg. Deviation (mm)	Std. Dev. Of Deviations (mm)	RMS Of Plane Fit (mm) Note: Stated instrument accuracy = 10 mm
Alum. pts to Sp. plane	0	Low	5.2	6.9	5.2
Sp. pts. to alum. plane	0	Low	-3.5	6.9	4.9
Alum. pts to Sp. plane	0	High	6.4	6.8	5.1
Sp. pts. to alum. plane	0	High	-0.8	7.0	5.1
Alum. pts to Sp. plane	30	Low	4.5	7.1	4.9
Sp. pts. to alum. plane	30	Low	-4.0	6.7	4.9
Alum. pts to Sp. plane	30	High	8.3	6.8	4.9
Sp. pts. to alum. plane	30	High	-3.3	6.5	4.9

Type of deviation	AOI (°)	Density	Avg. Deviation (mm)	Std. Dev. Of Deviations (mm)	RMS Of Plane Fit (mm) Note: Stated instrument accuracy = 10 mm
Alum. pts to Sp. plane	60	Low	3.3	4.5	3.9
Sp. pts. to alum. plane	60	Low	-3.0	4.2	4.0
Alum. pts to Sp. plane	60	High	1.2	4.2	3.8
Sp. pts. to alum. plane	60	High	-3.4	4.0	3.9
Alum. pts to Sp. plane	-30	Low	4.3	6.6	4.9
Sp. pts. to alum. plane	-30	Low	-3.2	6.7	4.9
Alum. pts to Sp. plane	-30	High	3.6	6.3	5.0
Sp. pts. to alum. plane	-30	High	-3.1	6.4	4.8
Alum. pts to Sp. plane	-60	High	-0.2	3.3	3.5
Sp. pts. to alum. plane	-60	High	-2.4	3.7	3.2

Table. 4. Instrument 4 - Deviations of points to the fitted plane. Data shown in red indicates the absolute value of the average deviation is greater than or equal to the RMS of the plane fit.

Type of deviation	AOI (°)	Avg. Deviation (mm)	Std. Dev. Of Deviations (mm)	RMS Of Plane Fit (mm) Note: Stated instrument accuracy = 0.035 mm
Alum. pts to Sp. plane	0	-0.0914	0.0856	0.0678
Sp. pts. to alum. plane	0	-0.0567	0.0949	0.0596
Alum. pts to Sp. plane	30	-0.1365	0.0765	0.0662
Sp. pts. to alum. plane	30	-0.0831	0.1044	0.0317
Alum. pts to Sp. plane	60	-0.1526	0.1301	0.0596
Sp. pts. to alum. plane	60	0.0561	0.1039	0.0424

3. DISCUSSION AND FINDINGS

In Tables 1 to 4, if the average deviation was less than the RMS of the plane fit, then the penetration of the Spectralon target could not be determined as it lay within the noise of the plane fit. In such cases, the penetration was considered to be insignificant. The RMS values of the plane fits for Instrument 4 were, for most of the cases, greater than the stated instrument accuracy. The RMS values of the plane fits for Instruments 1, 2 and 3 were less than the stated instrument accuracies.

In Table 1 (Instrument 1), in 6 (shown in red) out of 10 cases (60 %), the average deviation was greater than or equal to the RMS of the plane fit. The most conservative estimate of the target penetration is about 0.2 mm (the maximum average deviation).

In Table 2 (Instrument 2), in 20 of 20 cases (100 %), the average deviation was less than the RMS of the plane fit. Therefore, it is concluded that the target penetration, if any, is within the noise of the plane fit, and is not significant.

In Table 3 (Instrument 3), in 16 out of the 18 cases (89 %), the average deviation was less than the RMS of the plane fit. Therefore, it is concluded that the target penetration, if any, is within the noise of the plane fit, and not significant.

In Table 4 (Instrument 4), in 5 out of the 6 cases (83 %), the average deviation was greater than the RMS of the plane fit. In the 6th case, the average deviation was very close to the RMS of the plane fit. The most conservative estimate of the target penetration is about 0.2 mm (the maximum value rounded up).

Both Instruments 1 and 3 use a laser with a wavelength of 1550 nm. For Instrument 1, the findings indicate that there is penetration of about 0.2 mm into Spectralon. For Instrument 3, there was an indication of target penetration for about 10 % of the cases while target penetration was not discernible in the other 90 % due to the instrument noise.

The effect of AOI and point density on target penetration is shown in Fig. 8. From Fig. 8, Instruments 2 and 3, it is seen that the deviations are greater at an AOI of 0°, and the deviations, generally, decrease as the absolute value of the AOI increases (except for one instance - Instrument 3, AOI = 30, high density). The effect of point density on the deviation is mixed - again, it was expected that there would be no effect.

Based on the results from this limited experiment, we find that for Instruments 2 and 3 the penetration into a target made of Spectralon would not be discernible from the instrument noise. This is because the penetration depth is within the instrument noise. For Instruments 1 and 4, a very conservative estimate of the target penetration is 0.2 mm.
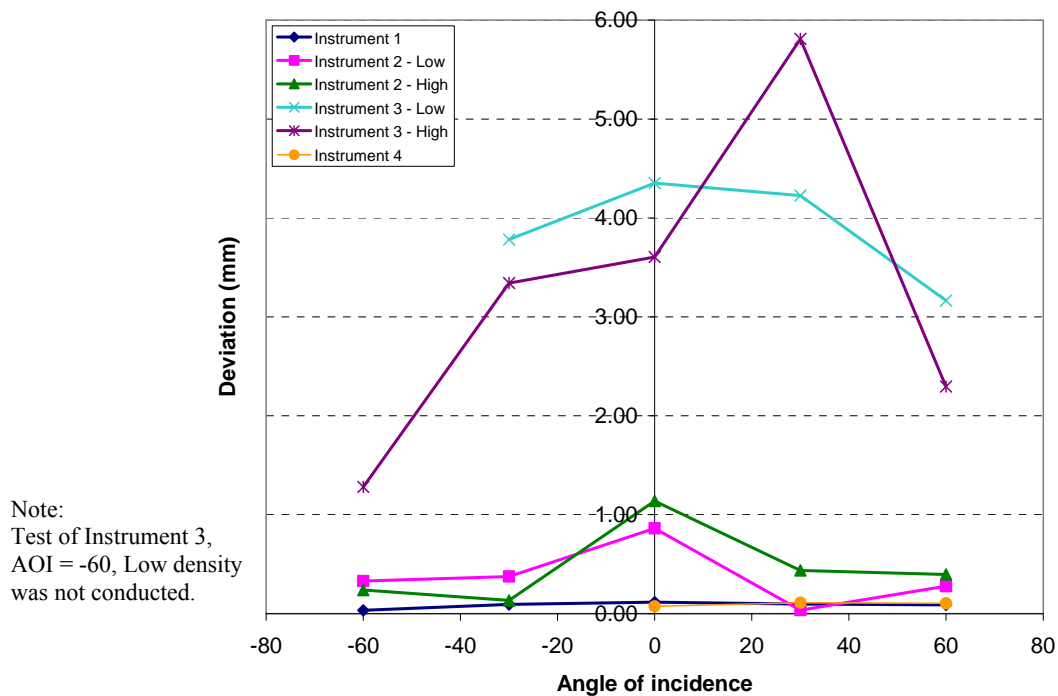

Note:
Test of Instrument 3,
AOI = -60, Low density
was not conducted.

Fig. 8.   Effect of angle of incidence and scan density on target penetration.

4.   ACKNOWLEDGEMENTS

REFERENCES

[1] Lytle, A. M., Cheok, G. S., and Saidi, K. S. [2007], "ASTM E-57 3D Imaging Systems Committee - An Update of the Standards Development Effort," in Laser Radar Technology and Applications XII, edited by G. W. Kamerman and M. D. Turner, Proceedings of SPIE, April.

[2] Cheok, G. S., Lytle, A. M., and Saidi, K. S. [2008], "ASTM E-57 3D Imaging Systems Committee: An Update," in Laser Radar Technology and Applications XIII, edited by M. D. Turner and G. W. Kamerman, Proceedings of SPIE, Vol. 6950, March 19-20, 2008.

[3] ASTM E2544-08b, "Standard Terminology for Three-Dimensional (3D) Imaging Systems", ASTM International, West Conshohocken, PA, www.astm.org.